Optimized engine transients

Tomas Nilsson
Department of
Electrical Engineering
Linköping University
Linköping, Sweden
Email: tnilsson@isy.liu.se

Anders Fröberg
Volvo CE
Eskilstuna, Sweden
Email: anders.froberg@volvo.com

Jan Åslund
Department of
Electrical Engineering
Linköping University
Linköping, Sweden
Email: jaasl@isy.liu.se

***Abstract*—Recent development has renewed the interest in drivetrain concepts which give a higher degree of freedom by disconnecting the engine and vehicle speeds. This freedom raises the demand for active control, which especially during transients is not trivial but of which the quality is crucial for the success of the drivetrain concept. This work attempts to analyze and explain the fuel optimal solution for the simplest drivetrain setup, which is an engine connected to a load which does not restrict the engine speed. This is made by using a Willan's model for the engine and deriving the fuel optimal solution during output power transients. The analysis is made with dynamic programming, Pontryagin's maximum principle and backward simulation under a static optimal line restriction. The analysis show that the optimal transients can be explained, visualized and, in simple cases, derived from phase planes of the engine speed and the Lagrange multiplier. In these cases the time needed for computation was reduced a factor > 1000 compared to dynamic programming. Restricting the engine to the static optimal line turns out to be very close to optimal, even during highly transient operation, while reducing the time needed for computation a factor $\gg 1000$.**

I. Introduction

A. Background and motivation

Faster, smaller and cheaper computers have created the opportunity for more intricate control of mechanical systems, or even introduction of new mechanical solutions that would have been unfeasible without a high level of control. In the field of vehicle engineering this can be seen in the recent diversification of drivetrain architectures [1]. The motivation for altering the drivetrain is often reduced fuel consumption, for environmental or economical reasons. It is easy to realize that the fuel consumption also depend on the driving cycle in which the vehicle operate [2]. For wheel loaders there are no standardized driving cycle, but it is clear that common wheel loader operation is highly transient [3] both in power requirement and vehicle speed. This is exemplified by the scaled engine output in Figure 1, which has been recorded during two consecutive loading cycles. The drivetrain of the in-production reference vehicle uses a diesel engine, a torque converter and an automatic gearbox. This solution has the advantage that it is mechanically robust since the torque converter provides some disconnection of the wheels from the engine, and that it automatically adapts to changes in torque. The drawback is that there is always some slip in the converter, which reduce efficiency.

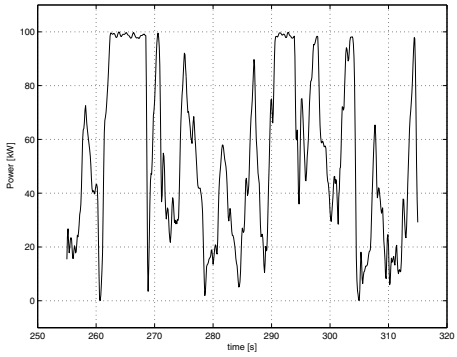

Fig. 1. Scaled engine output power of a wheel loader

There have been some work done on advanced wheel loader transmission control, but mainly in the fields of low level actuator control [4], autonomous vehicles [5] [6], and hybrid-electric powertrains with heuristic controls [7] [8]. There is also a vast amount of research on advanced on-road passenger vehicle drive trains. Most of these use heuristic control laws [9] [10] or some variant of the ECMS approach [11] [12]. Apart from these, there are articles such as [13] and [14] in which the optimal trajectory is derived, but not sufficiently examined. In [15] a thorough investigation of the optimal solution is made, but only for a fully stochastic future load.

There are several reasons for studying the optimal trajectory of vehicle operation, even though direct application of the solution would require perfect prediction of future operating conditions. In the case of hybrid electric vehicles with a simplified battery model, the optimization results in a single cycle-specific parameter which can be used in a causal controller, this is know as the ECMS [16]. Since it generally is optimal to operate at a stationary point during static conditions, the online optimization will in general only require prediction at transients, and then with a short horizon. Some proposals on how to achieve this can be found in [17] [18] [19]. In case the vehicle is made autonomous, as proposed by [5] [6], the controller may also inform the optimizer about upcoming actions.

The extremely transient operation of wheel loaders, along with new possibilities of realizing optimal operation, motivates further examination of optimal trajectories during transients.

B. Problem outline

Transmissions that enables higher efficiency through higher controllability are for example belt type CVTs or hydrostatic or electric drives. These can all be configured in numerous ways to emphasize desired properties. This makes it impossible to make a general analysis that includes any detail of the transmission. Since transients are a fundamental part of wheel loader usage, the goal of this paper is to gain deeper understanding of the mechanisms behind the optimal solution to transients. Therefore the aim is understanding the optimal transient engine operation, without regarding restrictions imposed by the transmission. This is done by subjecting the engine model to a load in the form of a non-stationary output power, and use different methods for analyzing the fuel optimal solution.

II. Problem

A. Drivetrain setup

The system consists of a diesel engine connected to a load which does not restrict the engine speed, such as an electric generator. The engine is modeled by a Willan's model [20]. The actual Willan's parameters used here are based on a typical diesel engine in the $100kW$ maximum output power range. The transmission efficiency is not included in the analysis.

B. Problem statement

The problem studied in this paper is the minimization of the total amount of fuel, or fuel energy (1), consumed during a driving mission specified by the load power trajectory.

$$\min \int_0^T P_{m_f} \mathrm{d}t \tag{1}$$

The load power trajectory is assumed to be known. Based on this knowledge the optimal engine operating point trajectory is derived. Each load case is solved by dynamic programming, analyzed with Pontryagin's maximum principle and compared to the solution when the engine operating point is restricted to the static optimal line. The methods will be analyzed and compared under three load cases:

- Slow steps: 25kW(5s) - 80kW(5s) - 25kW(5s)
- Quick steps: 25kW(5s) - 80kW(0.8s) - 25kW(5s)
- True case: Engine output according to Figure 1

The slow steps are made so that the engine has time to come to rest at a static point between the step up and the step down. In the quick steps the engine will not have time to settle in a static point. The true case exemplifies the engine output during two consecutive loading cycles, with the power scaled so that $\max P_{load} \approx 100kW$. For the load cases which require this, a lower bound of $500rpm$ for the engine has been used.

C. Engine model

The system is modeled as an inertia I_e which is affected by the engine torque T_e and a load torque. The load is defined by an externally specified power trajectory P_{load}.

$$\frac{d\omega_e(t)}{dt} \cdot I_e = T_e(t) - \frac{P_{load}(t)}{\omega_e(t)} \tag{2}$$

From here on t dependency will be omitted in the equations. The relation between injected fuel and engine torque is described by a Willan's model [20]

$$T_e = e \cdot A \cdot m_f - T_{loss} \tag{3}$$

in which m_f is fuel mass per injection, ω_e is engine speed

$$A = \frac{q_{lhv} n_{cyl}}{2\pi n_r} \tag{4}$$

$$e = e_0 - e_1 m_f \tag{5}$$

$$e_0 = e_{00} + e_{01}\omega_e + e_{02}\omega_e^2 \tag{6}$$

$$e_1 = e_{10} + e_{11}\omega_e \tag{7}$$

$$T_{loss} = T_{L0} + T_{L2}\omega_e^2 \tag{8}$$

in which q_{lhv} is the lower heating value, n_{cyl} is the number of cylinders, n_r is the number of strokes per injection and $e_{00}, e_{01}, e_{02}, e_{10}, e_{11}, T_{L0}, T_{L2}$ is the Willan's parameters. These are fitted against a typical wheel loader engine in the $100kW$ range. The engine efficiency is defined as the mechanical output power divided by the fuel input power

$$e_{tot} = \frac{P_e}{P_{m_f}} = \frac{T_e\omega_e}{\omega_e A m_f} = e_0 - e_1 m_f - \frac{T_{loss}}{A m_f} \tag{9}$$

The engine efficiency map given by equations (3) to (8) is presented in figure 3 along with the static optimal line. With the notation above, the problem (1) can be written as

$$\min \int_0^T A\omega_e m_f \mathrm{d}t \tag{10}$$

III. Method

A. Static optimal solution

The first step in analyzing optimal engine operation is the derivation of the static optimal operating points. This means maximizing (9) under static conditions, i.e. $\frac{d\omega_e(t)}{dt} = 0$. According to section II-C this can be formulated as

$$P_{load} = T_e\omega_e \tag{11}$$

which yields a static relation between ω_e, P_{load} and m_f:

$$m_f = \frac{e_0}{2e_1} - \sqrt{\left(\frac{e_0}{2e_1}\right)^2 - \frac{T_{loss}\omega_e + P_{load}}{A e_1 \omega_e}} \tag{12}$$

The maximum static efficiency can be found by solving

$$\frac{de_{tot}}{d\omega_e} = 0 \tag{13}$$

with (9) and (12), for each output power. This can not be easily solved analytically. Instead (9) is maximized numerically under (12) for a number of engine output powers.

B. Dynamic programming (DP)

Denote the discretized state X, the control U and the time t_k, with $k = 0, \ldots, N$. In the state, the control and the cost, the index $_k$ means (t_k). Then the dynamic programming algorithm [21] [22] can be written as

1: For $x_N \in X_N$, declare $J_N(x) = J_N$
2: **for** $k = N-1, \ldots, 1$ **do**
3: For each $x_k \in X_k$, simulate (2) for t_k to t_{k+1} for all $u \in U$ to find $x_{k+1}(x_k, u)$
4: For each $x_k \in X_k$

$$J_k(x_k) = \min_{u \in U}(Ax_k u\mathrm{d}t + \tilde{J}_{k+1}(x_{k+1})) \tag{14}$$

where $\tilde{J}_{k+1}(x_{k+1})$ is interpolated from $J_{k+1}(x \in X)$
5: **end for**
6: Select an initial engine speed $x_0^* = x_0$
7: **for** $m = 1, \ldots, N$ **do**
8: For x_{m-1}^*, simulate (2) for t_{m-1} to t_m for all $u \in U$ to find $x_m(x_{m-1}^*, u)$
9: Select

$$u_m^* = \underset{u \in U}{\operatorname{argmin}}(Ax_{m-1}^* u\mathrm{d}t + \tilde{J}_m(x_m)) \tag{15}$$

where $\tilde{J}_m(x_m)$ is interpolated from $J_m(x \in X)$
10: **end for**

The resulting $u^*(t_k)$, $x^*(t_k)$ is then the optimal trajectory when starting at x_0. In this work the simple final cost

$$J_N = \begin{cases} 0 & \text{if } x_N \geq \Omega \\ \infty & \text{if } x_N < \Omega \end{cases} \tag{16}$$

has been used. This method is simple to understand and guarantees global optimality. The drawback is that the method is computationally heavy due to the large number of short simulations that is made in step three of the algorithm. It is clear that the control and time discretization can not be too sparse if the continuous-space optimal solution is to be closely approximated. The success of the interpolation in steps four and nine depends on the size of X_k and the relation between x_k and J_k. In this problem J_k goes to infinity for high output powers combined with low engine speeds. This means that it is necessary to always have at least one grid point $x_{k+1} < x_{k+1}^*$ for which $J(x_{k+1})$ is finite or the result of the algorithm will be faulty. If at any point there is an infinite $J(x_{k+1})$, then $J(x_k)$ will be infinite unless there is an $x_{k+1}(x_k, u)$ that is not only higher than the x_{k+1} that give infinite cost but also higher than the next x in the grid. If the time discretization is made more dense, with unaltered state grid, the state derivative for moving from one x to a higher one increases. This means that with sparse X and dense t, the algorithm might be unable to increase x to clear an upcoming infinite $J(x_{k+1})$, and this infinite cost will get wrongfully propagated backwards in time as the algorithm proceeds. This means that the state discretization need to be dense in the region where $J(x)$ goes to infinity. Since this region is not known beforehand, this means that the state grid density has to be high throughout the entire state space and that increased time-grid density will also require increased state-grid density.

C. Pontryagin's maximum principle (PMP)

If we introduce the Hamiltonian

$$H = P_{m_f} + \lambda f(P_{load}, \omega_e, m_f) \tag{17}$$

where from equation (2) and (10), we get

$$P_{m_f} = A\omega_e m_f \tag{18}$$

$$f(P_{load}, \omega_e, m_f) = \frac{d\omega_e}{dt} = \frac{1}{I_e}(T_e - \frac{P_{load}}{\omega_e}) \tag{19}$$

which put together forms

$$H = A\omega_e m_f + \frac{\lambda}{I_e}(T_e - \frac{P_{load}}{\omega_e}) \tag{20}$$

then Pontryagin's maximum principle [23] [24] state that

$$\frac{\partial H}{\partial m_f} = A\omega_e + \frac{\lambda}{I_e}A(e_0 - 2e_1 m_f) = 0 \tag{21}$$

$$\frac{\partial H}{\partial \omega_e} = Am_f + \frac{\lambda}{I_e}(\frac{\partial T_e}{\partial \omega_e} + \frac{P_{load}}{\omega_e^2}) = -\frac{d\lambda}{dt} \tag{22}$$

in which

$$\frac{\partial T_e}{\partial \omega_e} = (e_{01} + 2e_{02}\omega_e - e_{11}m_f)Am_f - 2T_{loss2}\omega_e \tag{23}$$

must be fulfilled for a solution to (10) under the condition (2). Rewriting equation (21) gives

$$m_f = \frac{1}{2e_1}(\frac{\omega_e I_e}{\lambda} + e_0) \tag{24}$$

which is a static relation between m_f, ω_e and λ. Therefore (2) and (22) must hold all dynamics of the optimal engine operation. It also means that a solution of $\omega_e(t)$,$\lambda(t)$ can be easily translated to an $\omega_e(t)$,$T_e(t)$ trajectory, or vice versa. Unfortunately (2) and (22) can not be easily solved analytically, and since boundary conditions for λ in general are unknown, a numerical solution is not trivial. The λ-ω_e phase plane given by (2) and (22) reveals that for simple load trajectories there is a simple structure of the optimal solution.

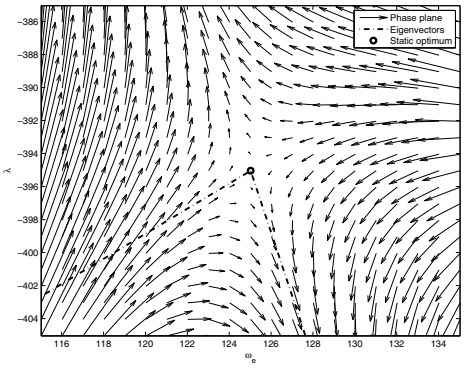

Fig. 2. Phase plane for $50kW$ load power, including eigenvectors and static optimal point

Figure 2 shows the phase plane for $P_{load} = 50kW$. It shows a saddle point at $\omega_e \approx 125rad/s \approx 1200rpm$, $\lambda \approx -395$, which according to (3) and (24) corresponds to $T_e \approx 400Nm$,

which is the static optimum for that output power. If the output power become constant for $\sim 1s$ or more (for this engine), the operating point must converge toward the static optimum, and do so from one of two directions; from higher output power or from lower output power. If there is an upcoming change in output power, the engine will leave the static optimum in one of two directions; toward higher or lower output power. Forward and backward simulations of (2) and (22) from the static optimum initiated by small disturbances in the positive and negative directions of the eigenvectors of the Jacobian

$$\begin{bmatrix} \frac{\partial \dot{\omega}_e}{\partial \omega_e} & \frac{\partial \dot{\omega}_e}{\partial \lambda} \\ \frac{\partial \dot{\lambda}}{\partial \omega_e} & \frac{\partial \dot{\lambda}}{\partial \lambda} \end{bmatrix} \tag{25}$$

can be used to find these paths. Since both ω_e and λ are continuous this mean that for simple output power trajectories the optimal path can be found by a simple combination of phase planes. In a step, for example, the engine must follow an 'out'-path of the earlier phase plane and an 'in'-path of the later phase plane, and where these paths cross the step must occur. This can be extended to somewhat more complicated load cases, as illustrated by the quick step load case, where two successive steps are made without letting the engine settle between the two. In this case there is a transition path in the intermediate output power phase plane that begins on the preceding 'out'-path and ends on the subsequent 'in'-path, and that requires the right amount of time. More complex load cases or such which requires low engine speeds, just like the true load case, would require the Hamiltonian (17) to be extended to incorporate the minimum engine speed bound.

D. Static optimal line restricted solution

One of the most intuitive methods of transient control is to keep the engine on the static optimal line, that is maintaining the $m_f(\omega_e)$ from the optimization in section III-A also during transients. Figure 3 and equation (2) show that this control give an unstable system for which there is a stationary point in $P_e = P_{load}$. This means that at a step in output power the system must already have exactly reached the new stationary point by a preceding divergence from the previous stationary point, initiated by a small disturbance. This approach is suboptimal since it disregards the energy stored in the inertia I_e. It is however a simple method and is worth comparing to the true transient optimal solution.

A method, which is robust and could be extended for finding this solution, is to use the previously described DP algorithm and simply add a penalty for deviating from the static optimal line. The drawback with this method is the computational effort it requires. Another method is based on the fact that with this method of control the engine speed becomes unstable. Because of this the system can easily be simulated backwards from an arbitrary terminal engine speed, for example using the Euler method according to (26) with $T_e(\omega_e)$ given by the static optimal line. This method has been used here.

$$\omega_{e,k-1} = \omega_{e,k} - \left(\frac{T_e(\omega_{e,k})\omega_{e,k} - P_{load}}{\omega_{e,k} I_e} \right) \mathrm{d}t \tag{26}$$

IV. Results

A. Static optimal solution

The static optimal line derived in section III-A is presented in Figure 3. This figure also shows constant output power lines with kW markings, efficiency curves according to equation (9), and a maximum engine torque bound.

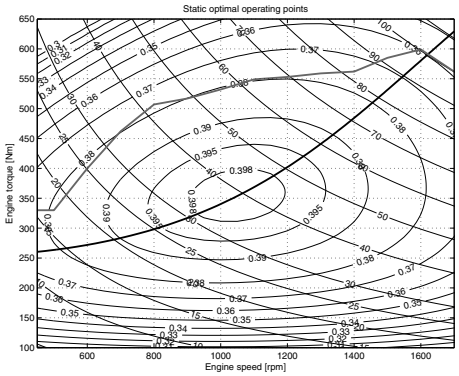

Fig. 3. Engine map showing efficiency curves with e_{tot} labels, output power with kW labels, the maximum engine torque and the static optimal line

B. Dynamic programming results

Figure 4 shows the engine map with operation point trajectory during the slow steps load case. The operating point moves in a counter clockwise direction; before the output power increase the operating point diverges toward high speed. When the output power is increased, the operating point motion changes direction and it converges toward the new static optimum by reducing the speed and increasing the torque. Before the output power reduction the engine speed will decrease, and at the step the motion will change direction and instead the torque will fall and the engine will converge to the new static optimum. Figure 5 shows the engine map with operation point trajectory for the true operating case displayed in Figure 1. Here too, the motion is counter-clockwise, but since the output power is never instantly changed but rather ramped, the direction changes to the lower right and the upper left is less pronounced.

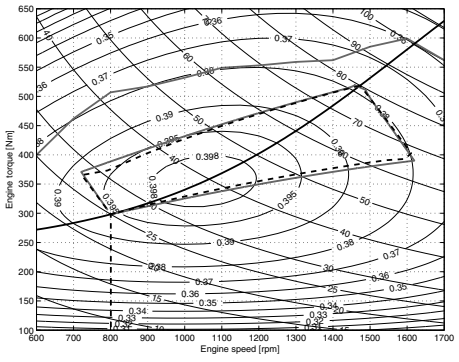

Fig. 4. Engine map movement during the slow steps load case, DP (dotted), PMP (continuous), the movement is counterclockwise

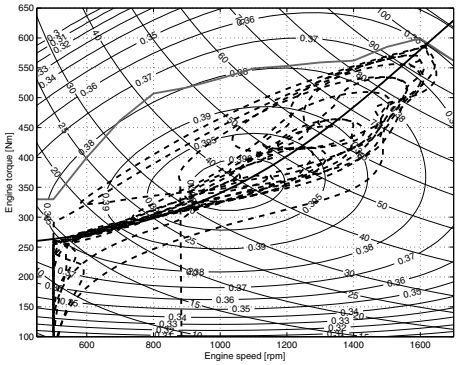

Fig. 5. Engine map movement during real case, counterclockwise movement

C. Pontryagin's maximum principle results

Figures 6 and 7 illustrates the phase-plane method for deriving the optimal trajectory for the slow steps load case. The figures show the phase planes for $25kW$ and $80kW$, with the static optimal line as a reference. Each figure shows one path in and one path out of the static optimal point. The unused paths are not displayed in any of the two phase planes. The optimal trajectory from one static optimal point to another is found by superposing the paths, as indicated by the shaded lines in the two figures. The λ-ω_e trajectories can be translated via equations (3) and (24) to trajectories in the T_e-ω_e engine map. The T_e-ω_e translation of the result is presented and

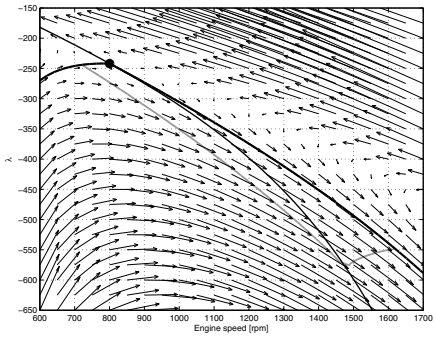

Fig. 6. $25kW$ λ-ω_e phase plane with one trajectory in and one out of the indicated static optimal operating point

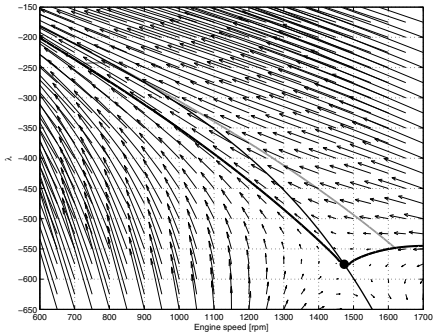

Fig. 7. $80kW$ λ-ω_e phase plane with one trajectory in and one out of the indicated static optimal operating point

compared to the DP-results in Figure 4. In the same way, Figure 8 shows the DP and PMP/phase-plane solutions to the quick step load case. The motion is described further in IV-B.

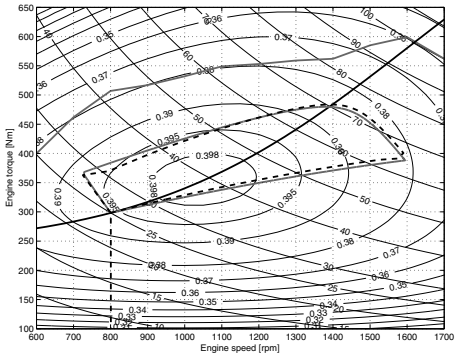

Fig. 8. Engine map trajectory during the quick steps load case, PMP (continuous) compared to DP (dotted) results, counterclockwise movement

D. Static optimal line restricted results

Figure 9 compares the true load case result when the engine operating point is restricted to the static optimal line, with the optimal trajectory (derived with DP, Figure 5). For visibility, since the difference between the two lines is small, only a seven second cutout is presented. Table I shows the increase in fuel consumption when restricting the engine to the static optimal line, compared to the optimum, for the three previously described cases. The static optimum corresponding to the terminal load has been used as terminal engine speed. This has also been used as Ω, and the resulting initial speed as x_0, in the dynamic programming reference (see section III-B).

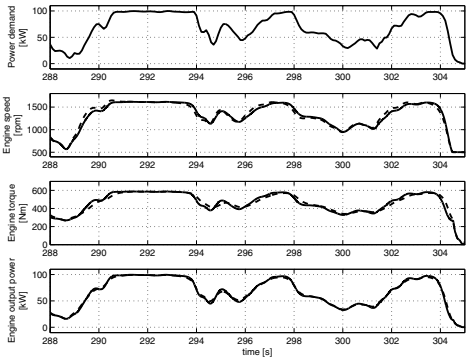

Fig. 9. Engine operation during real case, static optimal line restricted (continuous) compared to optimum (dotted) results

TABLE I
COST IN STATIC OPTIMAL LINE RESTRICTED SOLUTION

Load case	Cost increase
Slow steps	0.08%
Quick steps	0.15%
Real case	0.14%

V. Evaluation

The combination of (2), (22) and (24) provides an explanation of the behavior seen in numerical optimization of transient engine operation. A simple way of visualizing this is by phase planes, such as Figures 2, 6 and 7. For simple cases such as single or double steps it is easy to simulate these equations, and deriving the same result as provided by DP (Figures 4 and 8). For these cases the time required for solving the problems has been reduced by a factor > 1000. For sequences of multiple quick steps and/or ramps the method described for the quick steps load case (last part of section III-C) is applicable, even though the iteration will become more difficult. Applying this on a true load case is however complicated by the necessity of introducing inequality constraints, especially a lower bound on the engine speed. Introducing such bounds means that if an optimal solution according to section III-C violate any of these, that load case requires the Hamiltonian (17) to be extended [23] [24]. Figure 5, which may represent a common dynamic programming result for a true load case, shows that the general behavior follows that expected from the presentation of the phase planes; the operating point moves just as in Figure 4 in counterclockwise trajectories.

Figure 9 show that when the engine is restricted to the static optimal line the engine speed adopts somewhat slower to changes in output power. This causes the engine to spend more time in regions of lower efficiency. Still, the difference in efficiency is rather low, the increase in fuel consumption is lower than 0.2% in all analyzed cases. The computational complexity however has been drastically reduced, resulting in a computational time below even that for the PMP method. Also notice that that with this approach, the minimum engine speed bound is included in the static optimal line and hence pose no problem.

VI. Conclusions

PMP can be used for explaining and visualizing the optimal solutions for engine transients when using the Willan's approach in modeling the engine. For simple load cases it is even extremely efficient, compared to DP, for deriving these solutions . With a good iteration algorithm the method can be expected to work well also for more complex load cases, as long as the case start and end with constant loads. It is important to note that in this work the load trajectories have been selected so that the operating point does not violate any bounds, such as minimum engine speed. Such cases has not been solved with PMP since this would require (17) to be extended and not allow for the sole use of phase planes for visualization. If a solution had broken a boundary, this load case would require the model (17) to be extended [24].

Restricting the engine operating point to the static optimal line is suboptimal, but even in the highly transient true load case shown in this work the increase in fuel consumption compared to the optimum is less than 0.2%. The time for computing the solution however was reduced a factor $\gg 1000$ compared to dynamic programming.

References

[1] F. Buscemi, "Trends in automobile transmissions," *Gear technology*, vol. 23, pp. 24–26, 2006.

[2] X. Zeng, Q. Wang, and D. Song, "Direct statistical analyses of vehicle's fuel consumption based on driving cycles," *Journal of Hunan University Natural Sciences*, vol. 37, pp. 35–40, 2010.

[3] M. Starr, J. Buckingham, and C. Jackson, "Development of transient test cycles for selected nonroad diesel engines," *American Society of Mechanical Engineers, ICE Division*, vol. 32, 1999.

[4] J. Lennevi, "Hydrostatic transmission control," Ph.D. dissertation, Linkoping University, 1995.

[5] R. Ghabcheloo, M. Hyvnen, J. Uusisalo, O. Karhu, J. Jara, and K. Huhtala, "Autonomous motion control of a wheel loader," in *Proceedings of the ASME 2009 dynamic systems and control conference*. ASME, 2009, pp. 1339–1346.

[6] N. Koyachi and S. Sarata, "Unmanned loading operation by autonomous wheel loader," in *ICCAS-SICE 2009*. IEEE, 2009, pp. 2221–2225.

[7] R. Zhang, D. Carter, and A. Alleyne, "Multivariable control of an earthmoving vehicle powertrain, experimentaly validated in an emulated working cycle," in *2003 ASME international mechanical engineering congress*. ASME, 2003.

[8] S. Gramattico, A. Balluchi, and E. Cosoli, "A series-parallel hybrid electric powertrain for industrial vehicles," in *2010 IEEE vehicle power and propulsion conference*. IEEE, 2010, pp. 1–6.

[9] N. Srivastava and I. Haque, "A review on belt and chain continuously variable transmissions (cvt): dynamics and control," *Mechanism and machine theory*, vol. 44, pp. 19–41, 2009.

[10] S. Liu and B. Paden, "A survey of today's cvt controls," in *Proceedings of the 36th conference on decision and control*. IEEE, 1997, pp. 4738–4743.

[11] J. Liu and H. Peng, "Control optimization for a power-split hybrid vehicle," in *Proceedings of the 2006 american control conference*. IEEE, 2006, pp. 466–471.

[12] G. Paganelli, T. Guerra, S. Delprat, J. Santin, M. Delhom, and E. Combes, "Simulation and assessment of power control strategies for a parallel hybrid car," *Proceedings of the IMechE, Journal of automobile engineering*, vol. 214, pp. 705–717, 2000.

[13] D. Ambuhl, O. Sundstrom, A. Sciarretta, and L. Guzzella, "Explicit optimal control policy and its practical application for hybrid electric powertrains," *Control engineering practice*, vol. 18, pp. 1429–1439, 2010.

[14] R. Pfiffner, "Optimal operation of cvt-based powertrains," Ph.D. dissertation, ETH, Zurich, 2001.

[15] P. Rutquist, C. Brietholtz, and T. Wik, "An eigenvalue approach to infinite-horizon optimal control," in *Proceedings of the 16th IFAC world congress*. IFAC, 2005.

[16] A. Sciarretta and L. Guzzella, "Control of hybrid electric vehicles," *Control systems, IEEE*, vol. 27, pp. 60–70, 2007.

[17] B. Asadi and A. Vahidi, "Predictive cruise control: utilizing upcoming traffic signal information for improved fuel economy and reduced trip time," *IEEE transactions on control systems technology*, vol. 19, pp. 707–714, 2011.

[18] D. Mitrovic, "Reliable method for driving events recognition," *IEEE transactions on intelligent transportation systems*, vol. 6, pp. 198–205, 2005.

[19] A. Pentland and L. Andrew, "Modeling and prediction of human behavior," *Neural computation*, vol. 11, pp. 229–242, 1999.

[20] G. Rizzoni, L. Guzzella, and B. Baumann, "Unified modeling of hybrid electric vehicle drivetrains," *IEEE/ASME transactions on mechatronics*, vol. 4, pp. 246–257, 1999.

[21] R. Bellman, *Dynamic programming*. Princeton university press, 1957.

[22] D. Bertsekas, *Dynamic programming and optimal control*, 3rd ed. Athena scientific, 2005, vol. 1.

[23] L. Pontryagin, V. Boltyanskii, R. Gamkrelidze, and E. Mishchenko, *The mathematical theory of optimal processes*. Interscience publishers, 1962.

[24] A. Bryson, *Applied optimal control; optimization, estimation and control*. Taylor and Francis, 1975, ch. 2 & 3.